

FIRST-based survey of compact steep spectrum sources

V. Milliarcsecond-scale morphology of CSS objects

M. Kunert-Bajraszewska¹ and A. Marecki¹

Toruń Centre for Astronomy, N. Copernicus University, 87-100 Toruń, Poland

Received 8 September 2006; Accepted 7 March 2007

ABSTRACT

Aims. Multifrequency VLBA observations of the final group of ten objects in a sample of FIRST-based compact steep spectrum (CSS) sources are presented. The sample was selected to investigate whether objects of this kind could be relics of radio-loud AGNs switched off at very early stages of their evolution or possibly to indicate intermittent activity.

Methods. Initial observations were made using MERLIN at 5 GHz. The sources have now been observed with the VLBA at 1.7, 5 and 8.4 GHz in a snapshot mode with phase-referencing. The resulting maps are presented along with unpublished 8.4-GHz VLA images of five sources.

Results. Some of the sources discussed here show a complex radio morphology and therefore a complicated past that, in some cases, might indicate intermittent activity. One of the sources studied – 1045+352 – is known as a powerful radio and infrared-luminous broad absorption line (BAL) quasar. It is a young CSS object whose asymmetric two-sided morphology on a scale of several hundred parsecs, extending in two different directions, may suggest intermittent activity. The young age and compact structure of 1045+352 is consistent with the evolution scenario of BAL quasars. It has also been confirmed that the submillimetre flux of 1045+352 can be seriously contaminated by synchrotron emission.

Key words. galaxies: active, galaxies: evolution, quasars: absorption lines

1. Introduction

Following early hypotheses (Phillips & Mutel, 1982; Carvalho, 1985) suggesting that the gigahertz-peaked spectrum (GPS) and compact steep spectrum (CSS) could be young objects, Readhead et al. (1996) proposed an evolutionary scheme unifying three classes of radio-loud AGNs (RLAGNs): symmetric GPS objects – CSOs (compact symmetric objects); symmetric CSS objects – MSOs (medium-sized symmetric objects) and large symmetric objects (LSOs). In this scheme GPS/CSO sources with linear sizes less than 1 kpc¹ would evolve into CSS/MSOs with subgalactic sizes (<20 kpc) and these in turn would eventually become LSOs during their lifetimes. Two pieces of evidence definitely point towards GPS/CSS sources being young objects: lobe proper motions (up to 0.3c) giving kinematic ages as low as ~10³ years for CSOs (Owsianik et al., 1998; Giroletti et al., 2003; Polatidis & Conway, 2003) and radiative ages typically ~10⁵ years for MSOs (Murgia et al., 1999). Although these AGNs are small-scale objects, in some cases CSO/GPS sources are associated with much larger radio structures that extend out to many kiloparsecs. In these cases, it has been suggested that the CSO/GPS stage represents a period of renewed activity in the life cycle of the AGN (Stanghellini et al., 2005, and references therein). Reynolds & Begelman (1997) have also proposed a model in which extragalactic radio sources are intermittent on timescales

of ~10⁴–10⁵ years. Following the above scenarios and also an earlier suggestion by Readhead et al. (1994) and O’Dea & Baum (1997) that there exists a large population of compact, short-lived objects, Marecki et al. (2003, 2006) concluded that the evolutionary track proposed by Readhead et al. (1996) is only one of many possible tracks. A lack of stable fuelling from the black hole can inhibit the growth of a radio source, and consequently it will never reach the LSO stage, at least in a given phase of its activity.

Observational support for the above ideas has been provided by Gugliucci et al. (2005). They calculated the kinematic ages for a sample of CSOs with well-identified hotspots. It appears that the kinematic age distribution drops sharply above ~500 years, suggesting that in many CSOs activity may cease early. It is, therefore, possible that only some of them evolve any further. Our observations have shown that young, fading compact sources do indeed exist (Kunert-Bajraszewska et al., 2005; Marecki et al., 2006; Kunert-Bajraszewska et al., 2006, hereafter Papers II, III, and IV, respectively). A double source, 0809+404, described in Paper IV is our best example of a very compact – i.e. very young – fader. The VLBA multifrequency observations have shown it to have a diffuse, amorphous structure, devoid of a dominant core and hotspots. Giroletti et al. (2005) have analysed the properties of a sample of small-size sources and found a very good example of a kiloparsec-scale fader (1855+37). It is to be noted that re-ignition of activity in compact radio sources is not ruled out. In this paper – the fifth and the last of the series – VLBA observations of 10 CSS and CSO sources that are potential candidates for compact faders or objects with intermittent activity are presented. One of these sources, 1045+352, is of particular interest not only because it

Send offprint requests to: M. Kunert-Bajraszewska
e-mail: magda@astro.uni.torun.pl

¹ For consistency with earlier papers in this field, the following cosmological parameters have been adopted throughout this paper: $H_0=100 \text{ km s}^{-1} \text{ Mpc}^{-1}$ and $q_0=0.5$. Throughout this paper, the spectral index is defined such that $S \propto \nu^\alpha$.

has a puzzling radio structure, but it also appears to be a broad absorption line (BAL) quasar.

As their name somewhat suggests, BAL quasars have very broad, blue-shifted absorption lines arising from high-ionization transitions such as C IV, Si IV, N V, etc. (e.g. C IV 1549Å). They constitute $\sim 10\%$ of the optically selected radio-quiet quasars with the absorption arising from gas outflow at velocities up to $\sim 0.2c$ (Hewett & Foltz, 2003). In fact, BAL quasars have been divided into two categories, as 10% of them also show absorption troughs in low-ionization lines such as Mg II 2800Å. This group has been designated as LoBAL quasars and the others as HiBAL ones. The high ionization level and continuous absorption over a wide velocity range is hard to reconcile with absorption by individual clouds. Rather, they indicate that BAL regions exist in both BAL and non-BAL quasars and evidence, accumulated from optically selected BAL quasars, indicates an orientation hypothesis to explain their nature. It would appear that BAL quasars are normal quasars seen along a particular line of sight, e.g. a line of sight skimming the edge of the accretion disk or torus (Weymann et al., 1991; Elvis, 2000). Murray et al. (1995) have proposed a model in which the line of sight to a BAL quasar intersects an outflow or wind that is not entirely radial, e.g. an outflow that initially emerges perpendicular to the accretion disk and is then accelerated radially.

For quite a long time it was believed that BAL quasars were never radio-loud. This view was challenged by Becker et al. (1997), who discovered the first radio-loud BAL quasar when using the VLA FIRST survey to select quasar candidates. Five radio-loud BAL quasars were then identified in NVSS by Brotherton et al. (1998). Since then, the number of radio-loud BAL QSOs has increased considerably (Becker et al., 2000; Menou et al., 2001), following identification of new quasar candidates selected from the FIRST survey. Most of the BAL quasars in the Becker et al. (2000) sample tended to be compact at radio frequencies with either a flat or steep radio spectrum. Those with steep spectra could be related to GPS and CSS sources. A variety of their spectral indices also suggested a wide range of orientations, contrary to the interpretation favoured from optically selected quasars. Moreover, Becker et al. (2000) indicated that the frequency of BAL quasars in their sample was significantly greater (factor ~ 2) than inferred from optically selected samples and that the frequency of BAL quasars appeared to show a complex dependence on radio loudness.

The radio morphology of BAL quasars is important because it can indicate inclination in BALs, and therefore yields a direct test of the orientation model. However, information about the radio structure of BAL quasars is still very limited. Prior to 2006, only three BAL quasars, FIRST J101614.3+520916 (Gregg et al., 2000), PKS 1004+13 (Wills et al., 1999), and LBQS 1138–0126 (Brotherton et al., 2002) were known to have a double-lobed FR II radio morphology on kiloparsec scales, although this interpretation was doubtful for PKS 1004+13 (Gopal-Krishna & Wiita, 2000). Recently, the population of FR II-BAL quasars has increased to ten objects (excluding PKS 1004+13) following the discoveries of Gregg et al. (2006) and Zhou et al. (2006), although some of these still require confirmation. Their symmetric structures indicate an “edge-on” orientation, which in turn supports an alternative hypothesis described as “unification by time”, with BAL quasars characterised as young or recently refuelled quasars (Becker et al., 2000; Gregg et al., 2000). There has been only one attempt (at 1.6 GHz with the EVN) to image radio structures of the smallest (and possibly the youngest) BAL quasars (Jiang & Wang, 2003)

from the Becker et al. (2000) sample. This paper presents high frequency VLBA images of another very compact BAL quasar — 1045+352, which makes it the BAL quasar with the best known radio structure to date.

2. The observations and data reduction

The five papers of this series are concerned with a sample of 60 candidates selected from the VLA FIRST catalogue (White et al., 1997)² which could be weak CSS sources. The sample selection criteria have been given in Kunert et al. (2002) (hereafter Paper I). All the sources were initially observed with MERLIN at 5 GHz and the results of these observations led to the selection of several groups of objects for further study with MERLIN and the VLA (Paper II), as well as the VLBA and the EVN (Papers III and IV). The last of those groups contains 10 sources that, because of their structures (very faint “haloes” or possible core-jet structures), were not included in the other groups as they were less likely to be candidates for faders. However, to complete the investigation of the primary sample, 1.7, 5, and 8.4-GHz VLBA observations of 10 sources listed in Table 1 together with their basic properties, were carried out on 13 November 2004 in a snapshot mode with phase-referencing.³ Each target source scan was interleaved with a scan on a phase reference source and the total cycle time (target and phase-reference) was ~ 9 minutes including telescope drive times, with ~ 7 minutes actually on the target source per cycle. The cycles for a given target-calibrator pair were grouped and rotated round the three frequencies, although the source 1059+351 was only observed at 1.7 GHz with the VLBA because of its very low flux density as measured at 5 GHz by MERLIN (13 mJy).

The whole data reduction process was carried out using standard AIPS procedures but, in addition to this, corrections for Earth orientation parameter (EOP) errors introduced by the VLBA correlator also had to be made. For each target source and at each frequency, the corresponding phase-reference source was mapped, and the phase errors so determined were applied to the target sources, which were then mapped using a few cycles of phase self-calibration and imaging. For some of the sources a final amplitude self-calibration was also applied. IMAGR was used to produce the final “naturally weighted”, total intensity images shown in Figs. 1 to 10. Three of the ten sources (1056+316, 1302+356, 1627+289) were not detected in the 8.4-GHz VLBA observations, and 1425+287 has not been detected in any VLBA observations. Flux densities of the principal components of the sources were measured using the AIPS task JMFIT and are listed in Table 3.

In addition to the observations described above, unpublished 8.4-GHz VLA observations of five sources – 1056+316, 1126+293, 1425+287, 1627+289, 1302+356 – made in A-conf. by Glen Langston (first four objects) and Patnaik et al. (1992) have been included (Figs. 3, 5, 9, 10, and 7, respectively).

It was realised that because of poor u - v coverage at the higher frequencies, some flux density could be missing and the resultant spectral index maps were not considered to be reliable. Any calculation of spectral indices from the flux densities quoted in Table 3 should also be treated only as coarse approximations.

For 1045+352, 30-GHz continuum observations using the Toruń 32-m radio telescope and a prototype (two-element

² Official website: <http://sundog.stsci.edu>

³ Including this paper, the results of the observations of 46 sources out of 60 candidates from the primary sample have been published. The observations of 14 objects failed for different reasons.

Table 1. Basic parameters of target sources

Source Name (1)	RA h m s (2)	Dec ° ' " (3)	ID (4)	m_R (5)	z (6)	$S_{1.4\text{GHz}}$ mJy (7)	$\log P_{1.4\text{GHz}}$ W Hz ⁻¹ (8)	$S_{4.85\text{GHz}}$ mJy (9)	$\alpha_{1.4\text{GHz}}^{4.85\text{GHz}}$ (10)	LAS " (11)	LLS h ⁻¹ kpc (12)
1045+352	10 48 34.247	34 57 24.99	Q	20.86	1.604	1051	27.65	439	-0.70	~0.50	2.1
1049+384	10 52 11.797	38 11 43.83	G	20.76	1.018	712	27.04	205	-1.00	0.14	0.6
1056+316	10 59 43.236	31 24 20.59	G	21.10	0.307*	459	25.72	209	-0.63	0.50	1.4
1059+351	11 02 08.686	34 55 10.74	G	19.50	0.594*	702	26.52	252	-0.82	3.03	11.5
1126+293	11 29 21.738	29 05 06.40	EF	—	—	729	—	213	-0.99	0.79	—
1132+374	11 35 05.927	37 08 40.80	G	—	2.880	638	28.00	218	-0.86	~0.30	1.1
1302+356	13 04 34.477	35 23 33.93	EF	—	—	483	—	185	-0.77	~0.20	—
1407+369	14 09 09.528	36 42 08.06	q	21.51	0.996*	538	26.89	216	-0.73	~0.25	1.1
1425+287	14 27 40.281	28 33 25.78	EF	—	—	859	—	198	-1.18	0.75	—
1627+289	16 29 12.290	28 51 34.25	EF	—	—	526	—	162	-0.95	~0.65	—

Description of the columns: (1) source name in the IAU format; (2) source right ascension (J2000) extracted from FIRST; (3) source declination (J2000) extracted from FIRST; (4) optical identification: G - galaxy, Q - quasar, EF - empty field, q - star-like object, i.e. unconfirmed QSO; (5) red magnitude extracted from SDSS/DR5; (6) redshift; (7) total flux density at 1.4 GHz extracted from FIRST; (8) log of the radio luminosity at 1.4 GHz; (9) total flux density at 4.85 GHz extracted from GB6; (10) spectral index between 1.4 and 4.85 GHz calculated using flux densities in columns (7) and (9); (11) largest angular size (LAS) measured in the 5-GHz MERLIN image – in most cases, as a separation between the outermost component peaks, otherwise “~” means measured in the image contour plot; (12) largest linear size (LLS).

* photometric redshift extracted from SDSS/DR5

receiver) of the One-Centimeter Receiver Array (OCRA-p, Lowe et al., 2005) have also been made. The recorded output from the receiver was the difference between the signals from two closely-spaced horns effectively separated in azimuth so that atmospheric variations were mostly cancelled out. The observing technique was such that the respective two beams were pointed at the source alternately with a switching cycle of ~50 seconds for a period of ~6 minutes, thus measuring the source flux density relative to the sky background on either side of the source. The telescope pointing was determined from azimuth and elevation scans across the point source Mrk 421. The primary flux density calibrator that was used was the planetary nebula NGC 7027, which has an effective radio angular size of ~8 arcseconds (Bryce et al., 1997) and for which a correction of the flux density scale had to be made. However, as NGC 7027 was at some distance from the target source, the point source 1144+402 was used as a secondary flux density calibrator. Corrections for the effects of the atmosphere were determined from system temperature measurements at zenith distances of 0° and 60°.

3. Comments on individual sources

1045+352. The MERLIN and VLBA maps (Fig. 1) show this source to be extended in both the NE/SW and NW/SE directions. The central compact feature visible in all the maps is probably a radio core with a steep spectrum. The VLBA image at 1.7 GHz shows two symmetric protrusions – possibly jets – straddling the core in a NE/SW direction, the SW emission being weaker than in the NE. This structure is aligned with the NE/SW emission visible in the 5-GHz MERLIN image, but the more extended diffuse emission has been resolved out in the VLBA images. The 5-GHz VLBA image shows a core and a one-sided jet pointing to the East. Some compact features in a NE direction are also visible. The radio structure in the 8.4-GHz VLBA image is similar to that at 5 GHz: an extended radio core and a jet pointing in an easterly direction.

The observed radio morphology of 1045+352 could indicate a restart of activity with the NE/SW radio emission being the first phase of activity, now fading away, and the extension in the

NW/SE direction being a signature of the current active phase. However, the above is only one of a number of possible interpretations of the structure of 1045+352 – see further discussion in Sect. 4.

According to Sloan Digital Sky Survey/Data Release 5 (SDSS/DR5), 1045+352 is a galaxy at RA= 10^h48^m34^s.242, Dec= +34°57'24"/95, which is marked with a cross in the MERLIN map but the spectral observations carried out by Willott et al. (2002) have shown 1045+352 to be a quasar with a redshift of $z = 1.604$. It has been also classified as a HiBAL object based upon the observed very broad CIV absorption, and it is a very luminous submillimetre object with detections at both 850 μm and 450 μm (Willott et al., 2002).

The total flux of 1045+352 at 30 GHz measured by us using OCRA-p is $S_{30\text{GHz}} = 69 \text{ mJy} \pm 7 \text{ mJy}$, which gives a steep spectral index $\alpha = -1.01$ between 4.85 GHz and 30 GHz.

1049+384. The 5-GHz MERLIN image (Fig. 2) shows it as a triple core-jet structure with the brightest component resolved into a double structure extended in a NW/SE direction in the high resolution VLBA observations. The 1.7-GHz VLBA image shows four radio components (in agreement with Dallacasa et al., 2002), whereas the 5-GHz and 8.4-GHz VLBA maps show only three components. However, the 5-GHz VLBA image published by Orienti et al. (2004) shows all four components, and they suggest that the two western components and the two eastern ones are two independent radio sources. As pointed by Orienti et al. (2004), it is difficult to classify the object, although the idea that 1049+384 consists of two separate compact, double sources is not very plausible because of the very small separation, ~ 0.09" (0.4 kpc), between these two potential objects. Although the spectral index calculations are very uncertain, it is suggested that one of the eastern components at RA= 10^h52^m11^s.797, Dec= +38°11'44"/027 is a radio core (in agreement with Orienti et al., 2004) from which jets emerge alternately in opposite directions.

1049+384 is a galaxy with a redshift $z = 1.018$ (Riley & Warner, 1994), but according to Allington-Smith et al. (1988) the optical spectrum of 1049+384 shows intermediate properties between a galaxy and a quasar. The opti-

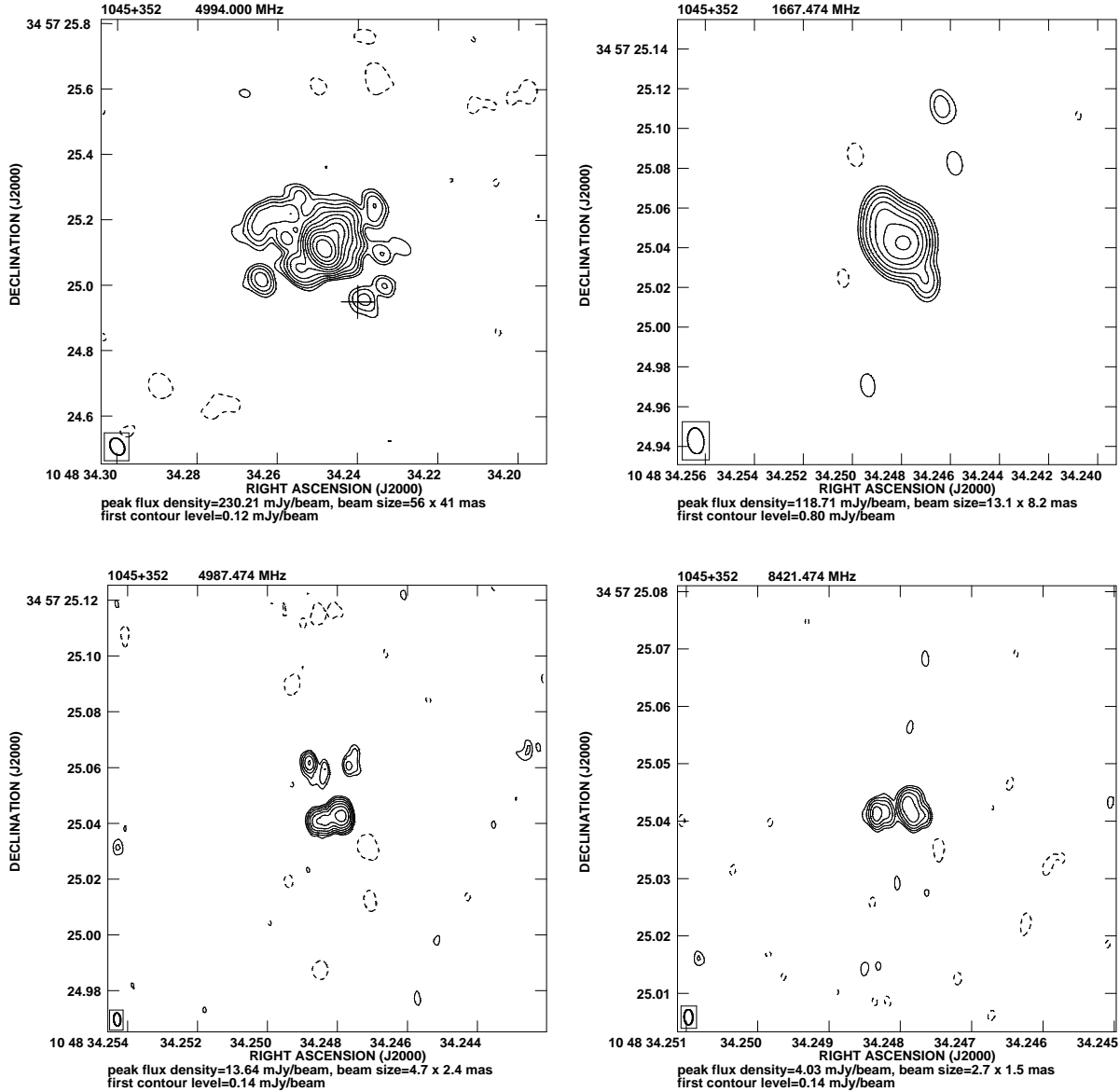


Fig. 1. The MERLIN 5-GHz (upper left) and VLBA 1.7, 5, and 8.4-GHz maps of 1045+352. Contours increase by a factor 2, and the first contour level corresponds to $\approx 3\sigma$. A cross indicates the position of an optical object found using the SDSS/DR5.

cal object was included in SDSS/DR5 (RA=10^h52^m11^s.802, Dec=+38°11′44″.00) and is marked in all maps with a cross.

1056+316. The 8.4-GHz VLA image (Fig. 3) shows this source to have a double structure that, in the 5-GHz MERLIN image, has been resolved into a radio core and probably a hotspot in a NW radio lobe. Both components are visible in the 1.7-GHz VLBA image, but neither has been detected in the higher frequency VLBA images. The two weak features on either side of the NW component in the 1.7-GHz VLBA image may be the remains of extended emission that has been resolved out.

The optical counterpart of 1056+316 was included in SDSS/DR5 (RA=10^h59^m43^s.145, Dec=+31°24′23″.31), together with a photometric redshift (Table 1). Its position is marked with a cross in 8.4-GHz VLA map.

1059+351. The 5-GHz MERLIN map (Fig. 4) shows a bright component that is probably a radio core, on almost opposite sides of which is emission from compact features (hotspots) within the two radio lobes. This structure agrees with the 1.4-

GHz VLA observations presented by Gregorini et al. (1988) and Machalski & Condon (1983). Their images clearly show an S-shaped morphology of 1059+351 with two very diffuse components, the brighter one resolved into a double structure in 5-GHz VLA observations (Machalski, 1998). One of these two components is the NW hotspot visible in the 5-GHz MERLIN map, and the second is probably a radio core visible in both the 5-GHz MERLIN and 1.7-GHz VLBA images.

The optical counterpart of 1059+351 was included in SDSS/DR5 (RA=11^h02^m08^s.727, Dec=+34°55′08″.79), together with a photometric redshift (Table 1). The position of the optical object is marked with a cross in all maps and is well correlated with the position of the radio core. Machalski (1998) also measured a photometric redshift for 1059+351, which is $z = 0.37$ and which differs from that in SDSS/DR5.

1126+293. The VLA 8.4-GHz and MERLIN 5-GHz maps (Fig. 5) show three radio components, the brighter one probably being the core that was resolved into a core-jet structure in

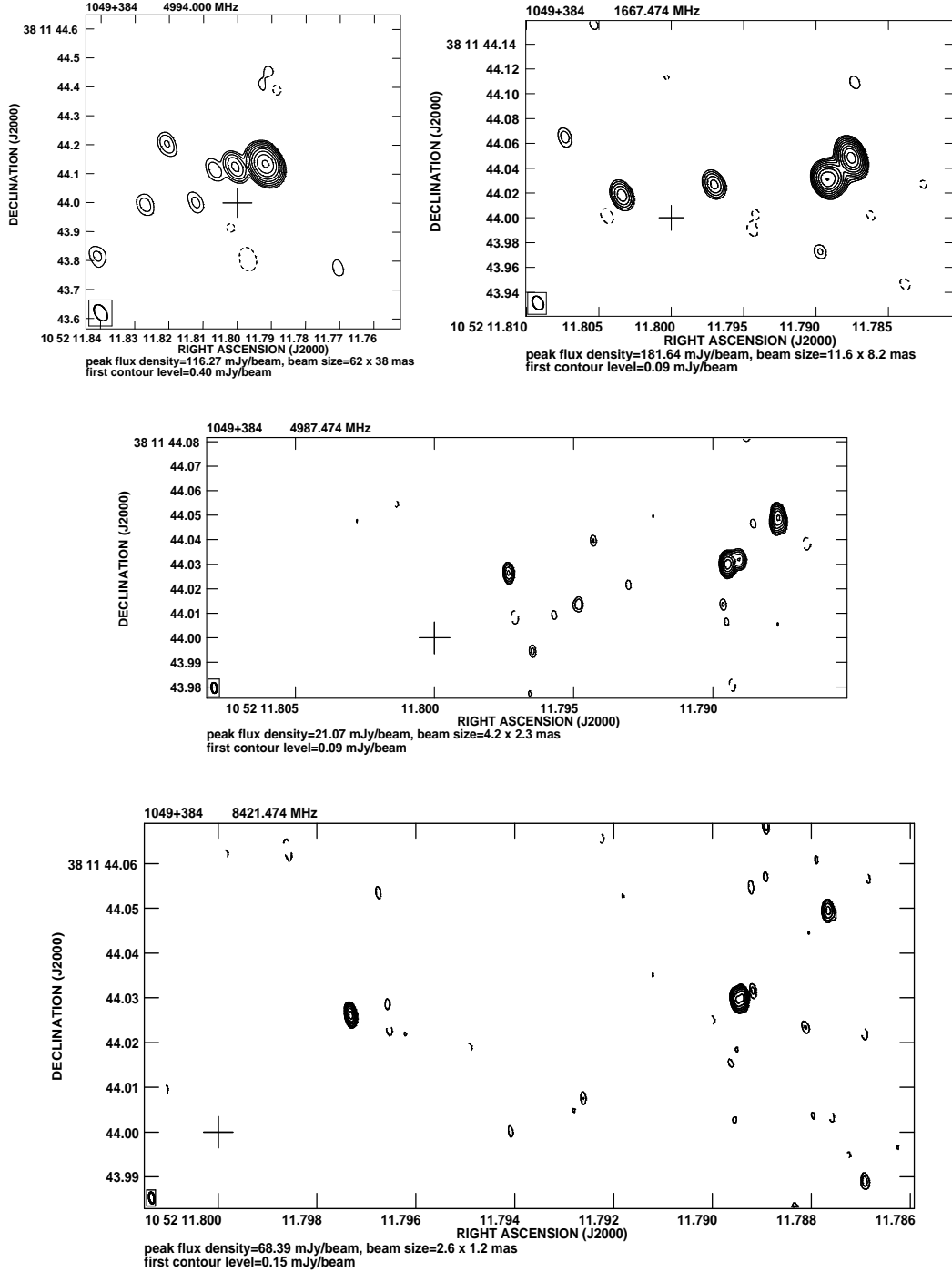


Fig. 2. The MERLIN 5-GHz (upper left) map and VLBA 1.7, 5, and 8.4-GHz maps of 1049+384. Contours increase by a factor 2, and the first contour level corresponds to $\approx 3\sigma$. Crosses indicate the position of an optical object found using the SDSS/DR5.

the 1.7-GHz VLBA image. The source was not detected in the 5 and 8.4-GHz VLBA observations.

1132+374. The 5-GHz MERLIN image shows (Fig. 6) a core-jet structure that was resolved into a triple CSO object in the 1.7-GHz VLBA image. The 5 and 8.4-GHz VLBA images show only two components: a hotspot in the NE lobe and a radio core. This source is identified with a very high redshift ($z = 2.88$) galaxy (Eales & Rawlings, 1996).

1302+356. This source was observed with the VLA at 8.4 GHz as a part of the JVAS survey (Patnaik et al., 1992). The result-

ing map shows a slightly extended EW object (Fig. 7). The 5-GHz MERLIN image shows this to be a double source, and the weak (~ 10 mJy) eastern component could be part of a jet. The bright component was resolved into a diffuse structure in the 1.7-GHz VLBA image. The 5-GHz VLBA image shows only a single component at the position of the maximum emission in the 1.7-GHz VLBA image, which is probably a radio core (Fig. 7). There is no trace of this source in the 8.4-GHz VLBA image.

1407+369. The 5-GHz MERLIN image shows a core-jet structure in a NW direction that is resolved into a core and jet in

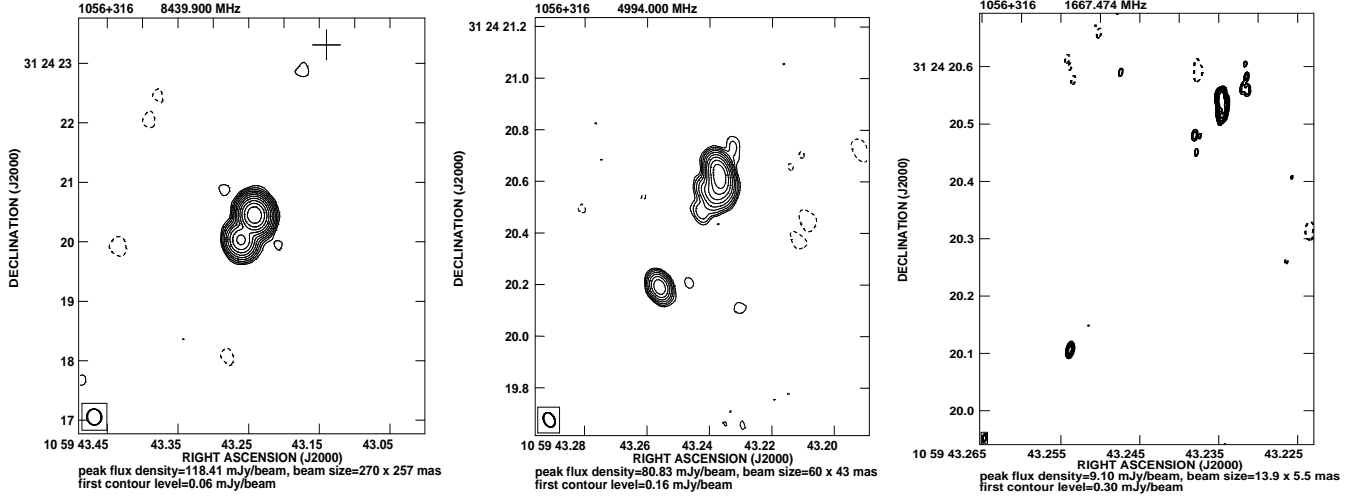


Fig. 3. The VLA 8.4-GHz map, MERLIN 5-GHz map, and VLBA 1.7-GHz map of 1056+316. Contours increase by a factor 2, and the first contour level corresponds to $\approx 3\sigma$. A cross on the VLA map indicates the position of an optical object found using the SDSS/DR5.

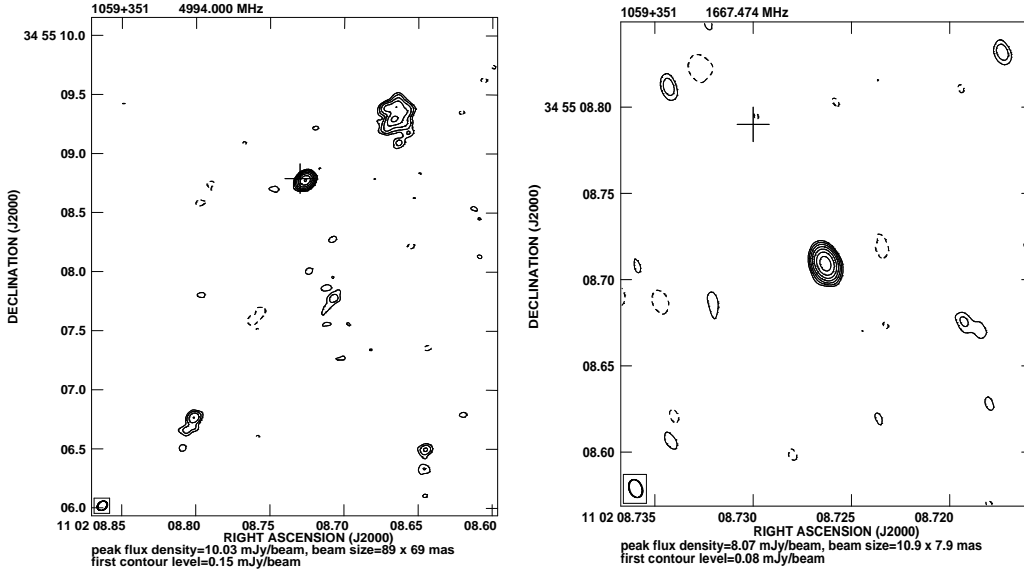


Fig. 4. The MERLIN 5-GHz map and VLBA 1.7-GHz map of 1059+351. Contours increase by a factor 2, and the first contour level corresponds to $\approx 3\sigma$. Crosses indicate the position of an optical object found using the SDSS/DR5.

all the VLBA maps (Fig. 8). The optical object was included in SDSS/DR5 (RA= $14^{\text{h}}09^{\text{m}}09^{\text{s}}.509$, Dec= $+36^{\circ}42'08''.15$) and is marked with a cross in all maps. The redshift quoted in Table 1 is photometric.

1425+287. Both the VLA 8.4-GHz and MERLIN 5-GHz images (Fig. 9) show a double structure for this source. The brighter component seems to be a radio core, although this cannot be confirmed because the source was not detected in the VLBA observations (Fig. 9).

1627+289. Both the VLA 8.4-GHz and MERLIN 5-GHz images (Fig. 10) show this source to have a core-jet structure. The 1.7-GHz VLBA image shows only the central extended feature that was resolved into a core-jet structure in the 5-GHz VLBA image. The source was not detected in the 8.4-GHz VLBA image.

4. Discussion

4.1. 1045+352 — a BAL quasar

1045+352 is a HiBAL quasar with a very reddened spectrum showing a CIV broad absorption system (Willott et al., 2002). Its projected linear size is only 2.1 kpc, which is consistent with the observation of Becker et al. (2000) that, amongst radio loud quasars, broad absorption lines are more commonly observed in the smallest radio sources.

It is a very luminous submillimetre object, which together with the template dust spectrum adopted by Willott et al. (2002), indicates this source to be a hyperluminous infrared quasar, with large amounts of dust in its host galaxy. Although 1045+352 is quite luminous at 151 MHz (2.88 Jy, Waldram et al., 1996), which suggests the presence of some extended emission and which, indeed, appears to be present in our MERLIN 5-GHz

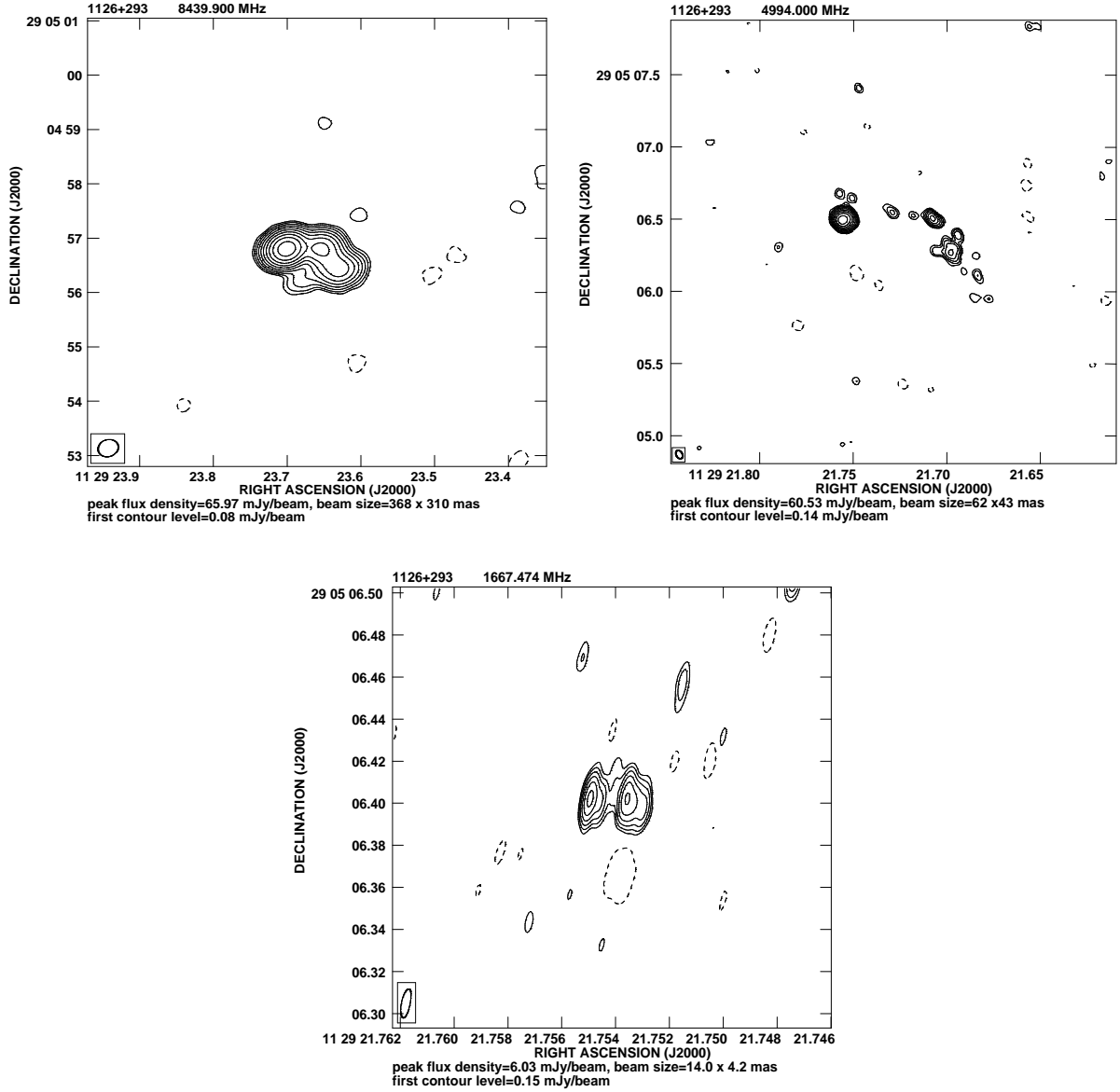


Fig. 5. The VLA 8.4-GHz map, MERLIN 5-GHz map and VLBA 1.7-GHz map of 1126+293. Contours increase by a factor 2, and the first contour level corresponds to $\approx 3\sigma$.

image, the VLBA maps show the radio structure to be dominated by jets and a core. The 30-GHz flux density of 1045+352 is also high, as would be expected from the VLBA structure. Consequently, there could be synchrotron contamination of the submillimetre flux. As shown by Blundell et al. (1999), either the first-order or second-order polynomials can accurately predict the shape of the radio spectrum. Both models have been applied to the radio data of 1045+352 taken from the literature and from this paper (Fig. 11), and show that a non-thermal component could constitute at least $\sim 40\%$ of the entire $850\mu\text{m}$ flux (the parabolic fit). The linear fit agrees with calculations based upon the 1.25 mm flux measured by Haas et al. (2006), who derived a value of 94% for the non-thermal component part of the detected $850\mu\text{m}$ flux. It has to be noted here that the linear fit should be treated as an upper limit for the synchrotron emission at submillimetre wavelengths, since the spectrum may steepen in the interval between 30 GHz and the SCUBA wavebands. However, the above can indicate values of infrared emission and dust mass of

1045+352 lower than estimated (Willott et al., 2002). This also appears to be consistent with the findings of Willott et al. (2003), who have shown that there is no difference between the submillimetre luminosities of BAL and non-BAL quasars, which suggest that a large dust mass is not required for quasars to show BALs.

The radio luminosity at 1.4 GHz is high (Table 1), making this source one of the most radio-luminous BAL quasars, with a value similar to that of the first known radio-loud BAL QSO with an FR II structure, FIRST J101614.3+520916 (Gregg et al., 2000). Following Stocke et al. (1992), a radio-loudness parameter, R^* , defined as the K -corrected ratio of the 5-GHz radio flux to 2500\AA optical flux (Table 2) was calculated. For this, a global radio spectral index, $\alpha_{\text{radio}} = -0.8$ and an optical spectral index, $\alpha_{\text{opt}} = -1.0$, were assumed, and the SDSS g' magnitude defined by Fukugita et al. (1996) was converted to the Johnson-Morgan-Cousins B magnitude using the formula given by Smith et al. (2002). Corrections were also made for intrinsic

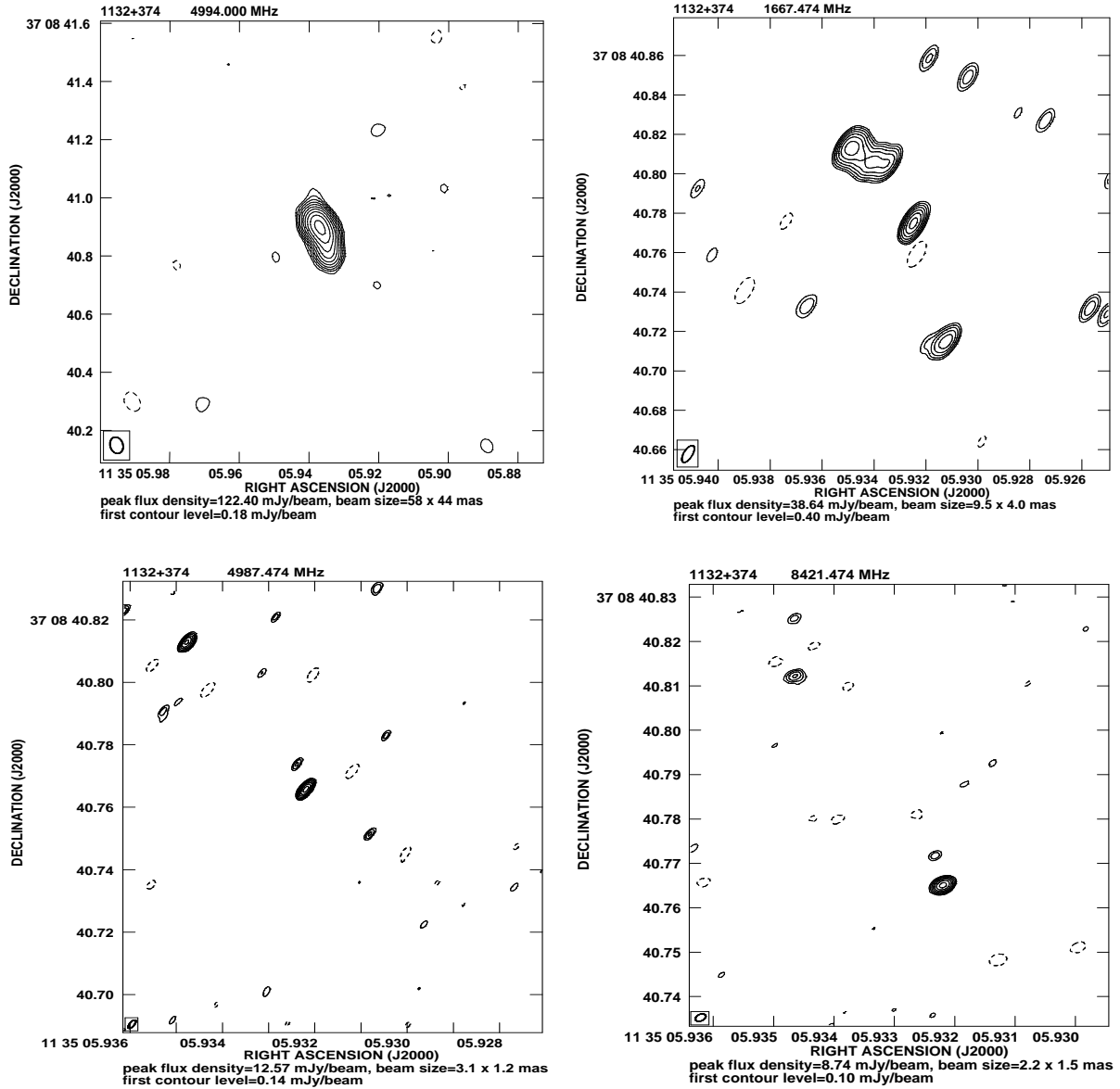


Fig. 6. The MERLIN 5-GHz (upper left) map and VLBA 1.7, 5, and 8.4-GHz maps of 1132+374. Contours increase by a factor 2, and the first contour level corresponds to $\approx 3\sigma$.

sic extinction (local to the quasar) calculated by Willott et al. (2002), who assumed a Milky-Way extinction curve. Even after correction, $\log(R^*) > 1$, which means that 1045+352 is still radio-loud object. The angle between the jet axis and the line of sight can be estimated using the core radio-to-optical luminosity ratio defined by Wills & Brotherton (1995) as $\log(R_V) = \log(L_{\text{core}}) + 0.4M_V - 13.69$, where L_{core} is a radio luminosity of the core at 5-GHz rest frequency (the core flux density at 5 GHz were taken from the VLBA image; see also Table 3), and M_V is the K -corrected absolute magnitude calculated using transformation equation $V = g' - 0.55(g' - r') - 0.03$ (Smith et al., 2002). From this, a value of ~ 3.2 has been obtained for 1045+352, implying an angle in the range $\theta \sim 10^\circ - 30^\circ$ for the jet in the observed asymmetric MERLIN 5-GHz radio morphology, and can explain the high value of the radio-loudness parameter. An assumption of $\theta = 20^\circ$ yields the deprojected linear size of the source of ~ 6 kpc. As shown by White et al. (2006), BAL QSOs are systematically brighter than non-BAL objects, which indi-

cates we are looking closer to the jet axis in quasars with BALs. Based upon the small inclination angles of their BAL quasars, Zhou et al. (2006) suggest that BAL features can be caused by polar disk winds. Also, Saikia et al. (2001) and Jeyakumar et al. (2005) found that the radio properties of CSS sources are consistent with the unified scheme in which the axes of the quasars are observed close to the line of sight. On the other hand, it has been shown (Saikia et al., 2001; Jeyakumar et al., 2005) that many CSS objects interact with an asymmetric medium in the central regions of their host galaxies, and this can cause the observed asymmetries. It is then likely that, also in the case of the CSS quasar 1045+352, the environmental asymmetries might play an important role. The jet power can be estimated from the relationship between the radio luminosity and the jet power given by Willott et al. (1999, Eq.(12)). However, because some of the flux density of the 1045+352 can be beamed, the calculations have to be treated as an approximation. Assuming the 151-MHz flux density, which accounts for the extended emis-

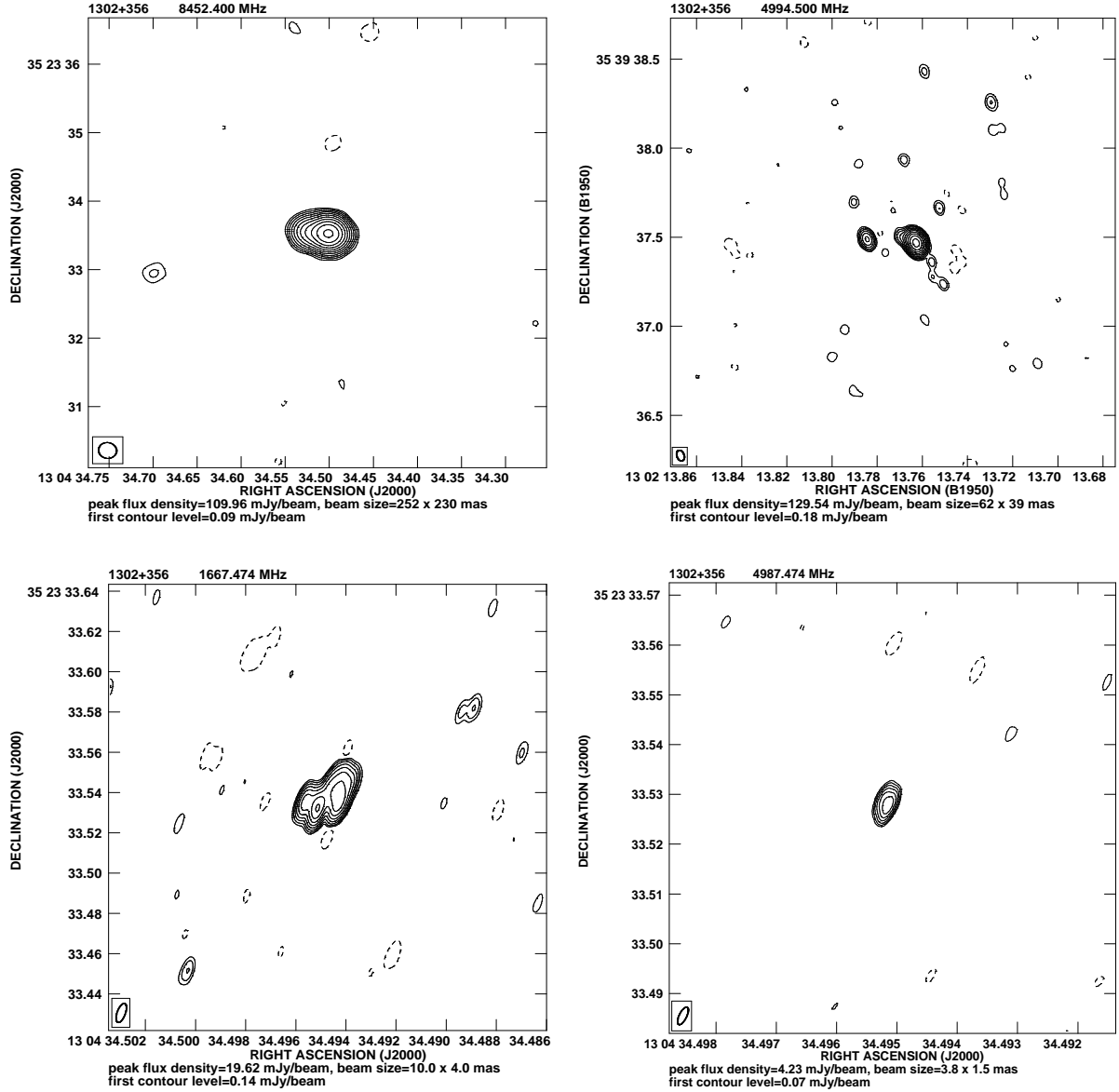


Fig. 7. The VLA 8.4-GHz map (upper left), MERLIN 5-GHz map (upper right) and VLBA 1.7 and 5-GHz maps of 1302+356. Contours increase by a factor 2, and the first contour level corresponds to $\approx 3\sigma$.

sion and the radio emission from the jets, the jet kinetic power is $Q_{jet} \sim 10^{44} \text{ erg sec}^{-1}$.

The projected linear size D of a radio quasar or radio galaxy can be approximately related to the time, from the triggering of activity, as the relationship between these variables is only weakly dependent upon the radio luminosity. Using the model of radio source evolution from Willott et al. (1999), the age of 1045+352 was estimated to be $\sim 10^5$ years (see also Willott et al., 2002; Rawlings et al., 2004). For the calculations we assumed: $\theta = 20^\circ$, $\beta = 1.5$, $c_1 = 2.3$, $n_{100} = 3000 \text{ e}^- \text{ m}^{-3}$, $a_0 = 100 \text{ kpc}$ (see Willott et al., 1999, for definitions). Both the MERLIN and VLBA high frequency images have revealed that two cycles of activity may have occurred during these $\sim 10^5$ years. The extended NE/SW emission is probably the remnant of the first phase of activity, which has been very recently replaced by a new phase of activity pointing in a NW/SE direction. It has been shown by Stanghellini et al. (2005) that the extended emission observed for small-scale objects can

be the remnants of an earlier period of activity in these sources. In the case of 1045+352, renewal of activity has been accompanied by a reorientation of the jet axis.

Several processes can be used to explain a jet reorientation in AGNs. There are strong observational and theoretical grounds for believing that accretion disks around black holes may be twisted or warped, and this can be caused by a number of possible physical processes. In particular, if there is a misalignment between the axis of rotating black hole and the axis of its rotating accretion disk, then the Lense-Thirring precession produces a warp in the disk. This process is called the Bardeen-Peterson effect (Bardeen & Peterson, 1975). According to Pringle (1997), disk warping can also be induced by internal instabilities in the accretion disk caused by radiation pressure from the central source.

A reorientation of the jet axis may also result from a merger with another black hole. Merritt & Ekers (2002) have shown that a rapid change in jet orientation can be caused by even a mi-

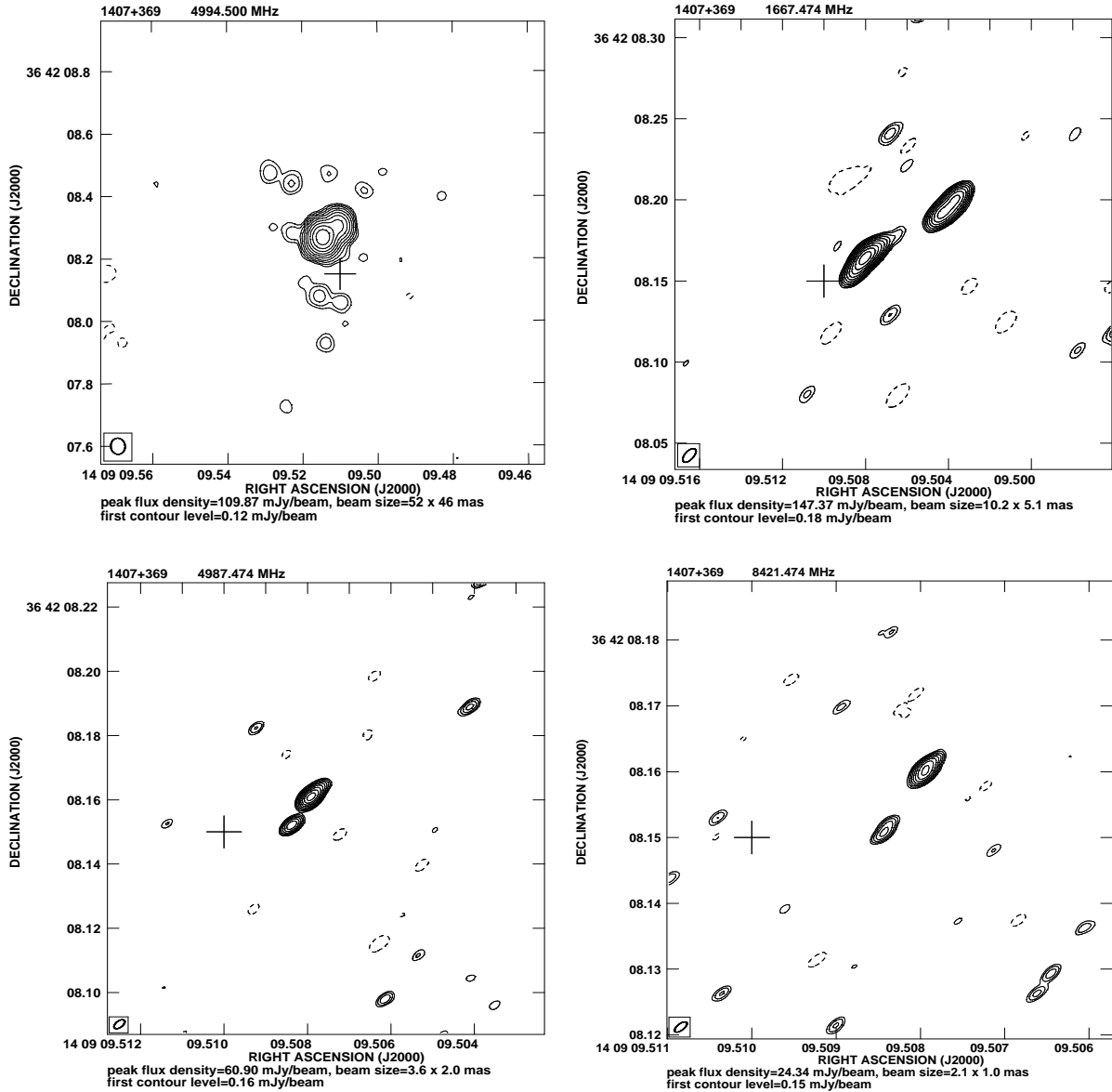


Fig. 8. The MERLIN 5-GHz map (upper left) and VLBA 1.7, 5, and 8.4-GHz maps of 1407+369. Contours increase by a factor 2, and the first contour level corresponds to $\approx 3\sigma$. Crosses indicate the position of an optical object found using the SDSS/DR5.

nor merger because of a spin-flip of the central active black hole arising from the coalescence of inclined binary black holes. According to Liu (2004), the Bardeen-Peterson effect can also cause a realignment of a rotating SMBH and a misaligned accretion disk, where the timescale of such a realignment $t < 10^5$ years. If it is assumed that the typical speed of advance of radio lobes of young AGNs is $v \sim 0.3c$ (Owsianik et al., 1998; Giroletti et al., 2003; Polatidis & Conway, 2003), then distorted jets of length, $tv < 10$ kpc for some CSS and GPS sources should be observed, although the character of these disturbances is not known. Liu (2004) shows that the interaction/realignment of a binary and its accretion disk leads to the development of X-shaped sources. 1045+352 is not a typical X-shaped source like 3C 223.1 or 3C 403 (Dennett-Thorpe et al., 2002; Capetti et al., 2002). However, according to Cohen et al. (2005) the realignment of a rotating SMBH followed by a repositioning of the accretion disk and jets is a plausible interpretation for misaligned radio structures, even if they are not conspicuously X-shaped.

It is likely that in young sources such as 1045+352, the gas has not yet settled into a regular disk following a merger event and that separate clouds of gas and dust reaching the very central regions of the source at different times disturb the stability of the accretion disk and affect the jet formation. Later, these clouds could cause a renewal of activity. Numerical simulations of colliding galaxies show that these usually merge completely after a few encounters in timescales up to $\sim 10^8$ years (Barnes & Hernquist, 1996). According to Schoenmakers et al. (2000), multiple encounters between interacting galaxies can cause interruptions of activity and lead to the many types of sources that are observed in a restarted phase, such as double-double radio galaxies. Nevertheless, it is unclear whether such encounters can cause jet reorientation. On the other hand, the dense medium of a host galaxy can frustrate the jets, and their collisions with the dense surrounding medium can cause rapid bends through large angles. In the case of 1045+352, the VLBA images at the higher frequencies seem to show a jet emerging in

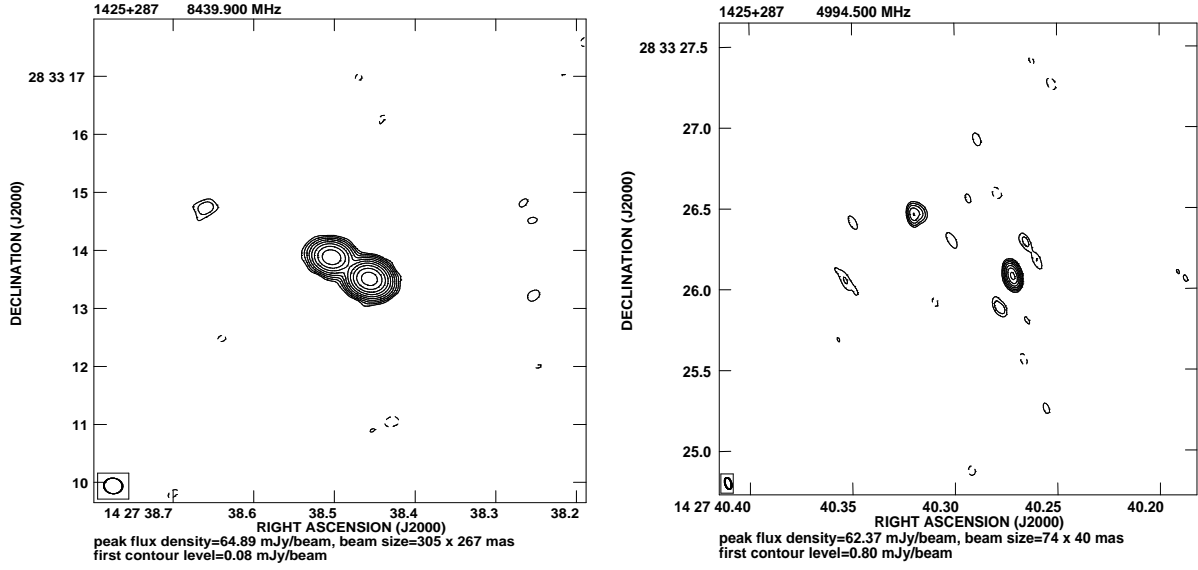


Fig. 9. The VLA 8.4-GHz map and MERLIN 5-GHz map of 1425+287. Contours increase by a factor 2, and the first contour level corresponds to $\approx 3\sigma$.

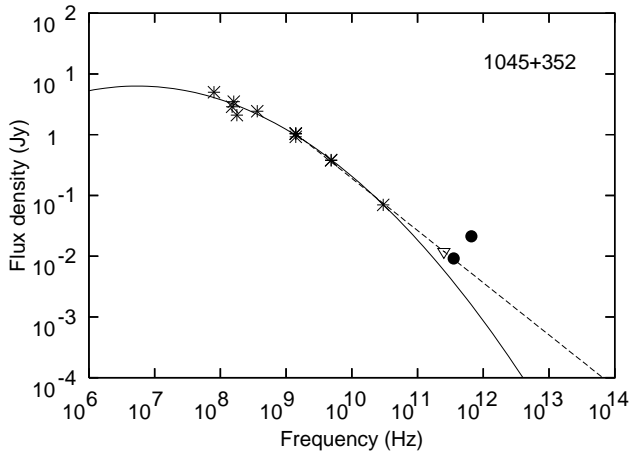


Fig. 11. Spectral Energy Distribution (SED) of 1045+352 from radio to submillimetre wavelengths. The errors are smaller than the size of the symbols; 1.25 mm point (Haas et al., 2006) is shown as a triangle, 850 μ m and 450 μ m points (Willott et al., 2002) are shown as filled circles, radio observations are shown as asterisks. The solid curve is the parabolic fit $f(x) = ax^2 + bx + c$ to all radio data (y_i), with $a = -0.14$, $b = 1.91$, $c = -5.68$, and reduced $\chi^2 = 12$. The dashed curve is the linear fit $f(x) = ax + b$ to radio data with $\nu > 1$ GHz, with $a = -0.86$, $b = 7.91$, and reduced $\chi^2 = 0.5$.

a S/SE direction, but being bent through $\sim 60^\circ$ to a NE direction in the lower resolution 1.7-GHz image. The MERLIN lower resolution 5-GHz image might indicate that the jet has been bent again and now emerges from the core in a NW direction.

It is difficult to find a convincing argument in favour of one of the above-mentioned alternatives or to rule any of them out based upon the extensive multifrequency data on 1045+352 presented here. However, if it is assumed that a merger is the most probable cause of the ignition and restart of activity in radio galaxies, this could mean that 1045+352 has undergone two merger events in a very short period of time ($\sim 10^5$), which is un-

Table 2. 1045+352 properties

Parameter	Value
u'	22.12
g'	21.38
r'	20.81
i'	20.14
z'	20.08
A_B	2.0
M_B	-22.05 (-24.05)
A_V	1.5
M_V	-22.83 (-24.33)
$\log(R^*)(\text{total})$	4.9 (4.1)
$\log(R^*)(\text{core})$	3.8 (3.0)

Notes: Optical photometry from SDSS, corrected for Galactic extinction. A_V taken from Willott et al. (2002). Quantities in parentheses are corrected for intrinsic extinction.

likely. More probable is that the ignition of activity in 1045+352 has occurred during a merger event that is, as yet, incomplete and that disturbed, misaligned radio jets result from the realignment of a rotating SMBH or intermittent gas injection that interrupts jet formation.

4.2. Other nine sources

Three sources from our sample (1126+293, 1407+369, 1627+289) show one- or two-sided core-jet structures, indicating that they are in an active phase of their evolution, although the core-jet structure of 1126+293 is controversial. Our images indicate that the western components are parts of the jet, which is possibly precessing or being bent by interactions with the interstellar medium. They could, however, also be hotspots of a radio lobe. Unfortunately, our high frequency VLBA observations are not sensitive enough to settle this problem. Three other sources (1056+316, 1132+374, 1425+287) have visible radio cores and parts of lobes or hotspots, indicating activity. 1132+374 is a CSO object. In the case of one source, 1059+351, the VLBA obser-

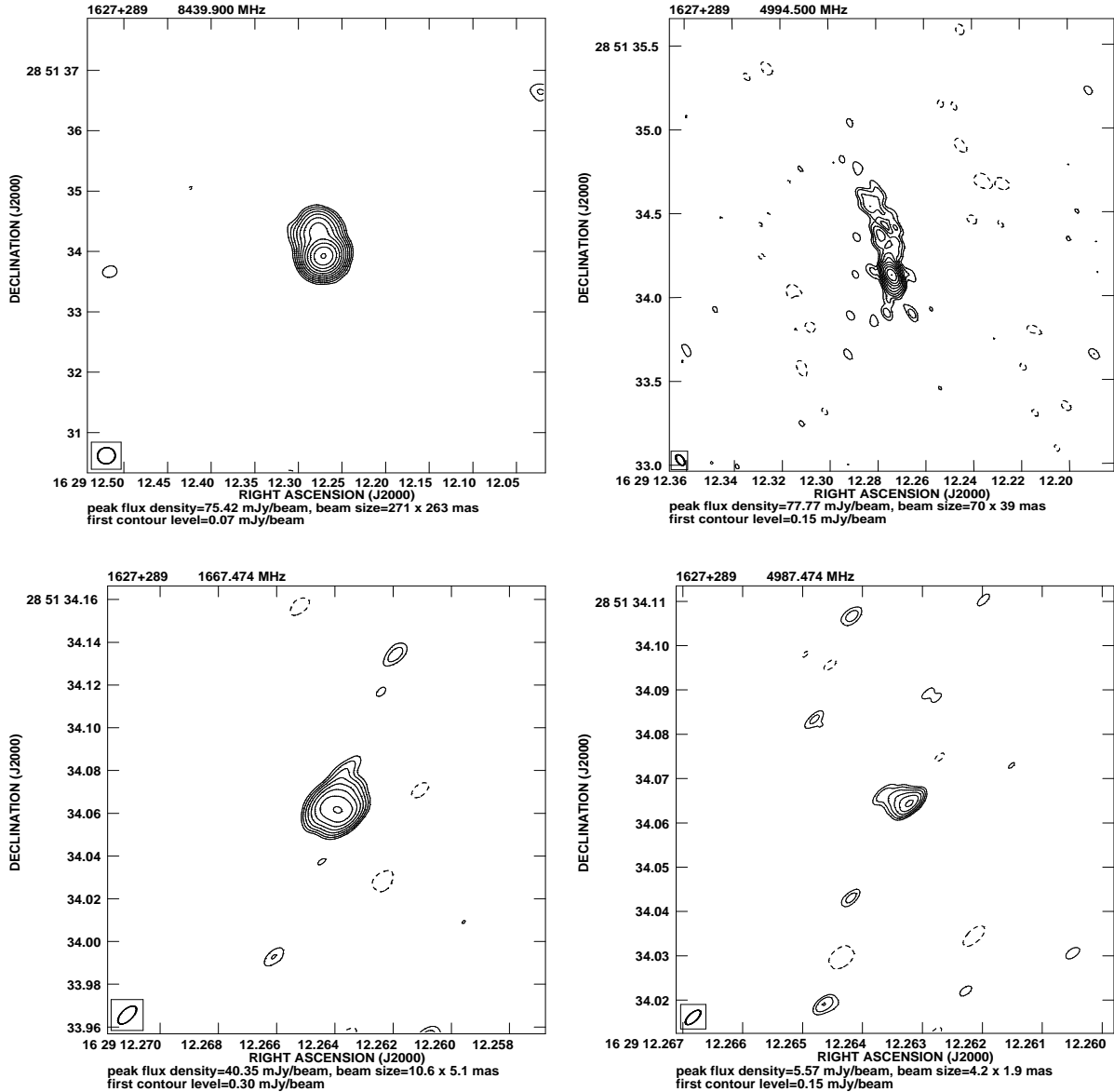


Fig. 10. The VLA 8.4-GHz map (upper left), MERLIN 5-GHz map (upper right), and VLBA 1.7 and 5-GHz maps of 1627+289. Contours increase by a factor 2, and the first contour level corresponds to $\approx 3\sigma$.

ations show only a radio core, although the 5-GHz MERLIN image of 1059+351 also shows remnants of the two radio lobes of its “S” shaped structure visible at the VLA resolutions (Machalski & Condon, 1983; Machalski, 1998). According to Taylor et al. (1996) and Readhead et al. (1996), “S” symmetry is observed in many compact sources and can be explained by precession of the central engine. 1059+351 is the largest source in our sample with a linear size of 45 kpc based upon its largest angular size measured from 1.46-GHz VLA image (Machalski & Condon, 1983).

The compact 1049+384 and 1302+356 steep spectrum sources appeared to be low-frequency variables (LFV) at 151 MHz with very high (≥ 0.99) probabilities that their variability is real (Minns & Riley, 2000). According to them, LFV objects are generally more compact than other CSS sources and tend to exhibit steeper spectra than typical CSS sources. This may be because of rapid spectral ageing, which might be ex-

pected for frustrated sources, or it might simply be because the sources are at very high redshifts.

5. Conclusions

VLBA, VLA, and MERLIN images of ten compact steep spectrum sources have been presented. One of these sources, 1045+352, is a very radio-luminous BAL quasar, whose complex structure suggests restarted activity. This may have resulted either from a merger event or from the infall of a cloud of gas, that had cooled in the halo of the galaxy into the core region of the source. The asymmetric radio jets of 1045+352 and the estimated angle suggest that some of the emission can be boosted, although the intrinsic asymmetries cannot be ruled out. It has also been confirmed that the $850\mu\text{m}$ flux of 1045+352 can be severely contaminated by synchrotron emission, which may suggest less than previously estimated values of infrared emission and dust mass. Most of the radio-loud BAL quasars detected to

Table 3. Flux densities of sources principal components from the VLBA observations

Source Name (1)	RA h m s (2)	DEC ° ' " (3)	S _{1.7GHz} mJy (4)	S _{5GHz} mJy (5)	S _{8.4GHz} mJy (6)	θ_1 mas (7)	θ_2 mas (8)	PA ° (9)
1045+352	10 48 34.248	34 57 25.044	303.2	–	–	15.0	11.0	60
	10 48 34.249	34 57 25.061	–	3.5	–	2.0	1.0	76
	10 48 34.248	34 57 25.041	–	21.8	7.1	7.0	1.0	101
	10 48 34.248	34 57 25.043	–	32.7	12.3	4.0	3.0	95
1049+384	10 52 11.803	38 11 44.018	13.6	–	–	3.0	1.0	14
	10 52 11.797	38 11 44.027	11.4	3.9	6.9	2.0	2.0	121
	10 52 11.789	38 11 44.031	182.1	33.6	12.9	8.0	1.0	119
	10 52 11.787	38 11 44.048	218.5	23.9	2.3	5.0	3.0	177
1056+316	10 59 43.254	31 24 20.106	8.8	–	–	0.9	0.1	7
	10 59 43.235	31 24 20.538	43.6	–	–	33.0	8.0	6
1059+351	11 02 08.726	34 55 08.709	8.1	–	–	0.7	0.3	124
1126+293	11 29 21.755	29 05 06.402	7.3	–	–	3.0	1.0	84
	11 29 21.753	29 05 06.401	10.4	–	–	13.0	4.0	53
1132+374	11 35 05.934	37 08 40.810	124.1	6.6	1.6	18.0	2.0	57
	11 35 05.932	37 08 40.775	36.3	13.8	9.4	2.0	0.4	8
	11 35 05.931	37 08 40.715	14.5	–	–	5.0	0.8	105
1302+356	13 04 34.495	35 23 33.534	46.8	5.9	–	11.0	6.0	97
	13 04 34.494	35 23 33.538	60.5	–	–	15.0	7.0	147
1407+369	14 09 09.504	36 42 08.195	81.0	1.9	–	17.0	3.0	138
	14 09 09.508	36 42 08.164	192.8	76.7	42.0	8.0	1.5	141
	14 09 09.508	36 42 08.152	–	9.5	4.8	0.7	0.2	140
1627+289	16 29 12.264	28 51 34.062	111.5	8.1	–	10.0	6.0	58

Description of the columns: (1) source name in the IAU format; (2) component right ascension (J2000) as measured at 1.7 GHz; (3) component declination (J2000) as measured at 1.7 GHz; (4) VLBA flux density in mJy at 1.7 GHz from the present paper; (5) VLBA flux density in mJy at 5 GHz from the present paper; (6) VLBA flux density in mJy at 8.4 GHz from the present paper; (7) deconvolved component major axis angular size at 1.7 GHz obtained using JMFIT; (8) deconvolved component minor axis angular size at 1.7 GHz obtained using JMFIT; (9) deconvolved major axis position angle at 1.7 GHz obtained using JMFIT. In the case the component is not visible in 1.7 GHz map the values for the last three columns are taken from the 5-GHz image.

date have very compact radio structures similar to GPS and CSS sources which are thought to be young. Therefore, the compact structure and young age of 1045+352 fit well to the evolutionary interpretation of radio-loud BAL QSOs.

According to the evolutionary model recently proposed by Lipari & Terlevich (2006), BAL quasars are young systems with composite outflows, and they are accompanied by absorption clouds. The radio-loud systems may be associated with the later stages of evolution, when jets have removed the clouds responsible for the generation of BALs. The effect of orientation could play a secondary role here. The above could explain the rarity of extended radio structures showing BAL features (Gregg et al., 2006).

Acknowledgements.

The VLBA is operated by the National Radio Astronomy Observatory (NRAO), a facility of the National Science Foundation (NSF) operated under cooperative agreement by Associated Universities, Inc. (AUI).

This research has made use of the NASA/IPAC Extragalactic Database (NED), which is operated by the Jet Propulsion Laboratory, California Institute of Technology, under contract with the National Aeronautics and Space Administration.

Use has been made of the Sloan Digital Sky Survey (SDSS) Archive. The SDSS is managed by the Astrophysical Research Consortium (ARC) for the Participating Institutions: The University of Chicago, Fermilab, the Institute for Advanced Study, the Japan Participation Group, The Johns Hopkins University, Los Alamos National Laboratory, the Max-Planck-Institute for Astronomy (MPIA), the Max-Planck-Institute for Astrophysics (MPA), New Mexico State University, University of Pittsburgh, Princeton University, the United States Naval Observatory, and the University of Washington.

We thank M. Gawroński for his help with the OCRA-p observations. The OCRA project was supported by the Polish Ministry of Science and Higher Education under grant 5 P03D 024 21 and the Royal Society Paul Instrument Fund.

We thank P.J. Wiita for a discussion and P. Thomasson for reading of the paper and a number of suggestions.

This work was supported by the Polish Ministry of Science and Higher Education under grant 1 P03D 008 30.

References

- Allington-Smith, J., R., Spinrad, H., Djorgovski, S., & Liebert, J. 1988, MNRAS, 234, 1091
- Bardeen, J. M., & Petterson, J. A. 1975, ApJ, 195, L65
- Barnes, J. E., & Hernquist, L. 1996, ApJ, 471, 115
- Becker, R. H., Gregg, M. D., Hook, I. M., et al. 1997, ApJ, 479, L93
- Becker, R. H., White, R. L., Gregg, M. D., et al. 2000, ApJ, 538, 72
- Blundell, K. M., Rawlings, S., & Willott, C. J. 1999, ApJ, 117, 677
- Brotherton, M. S., van Breugel, W., Smith, R. J., et al. 1998, ApJ, 505, L7
- Brotherton, M. S., Croom, S. M., De Breuck, C., Becker, R. H., & Gregg, M. D. 2002, AJ, 124, 2575
- Bryce, M., Pedlar, A., Muxlow, T., Thomasson, P., & Mellema, G. 1997, MNRAS, 284, 815
- Capetti, A., Zamfir, S., Rossi, P., et al. 2002, A&A, 394, 39
- Carvalho, J. C. 1985, MNRAS, 215, 463
- Cohen, A. S., Clarke, T. E., Ferretti, L., & Kassim, N. E. 2005, ApJ, 620, L5
- Dallacasa D., Tinti, S., Fanti, C., et al. 2002, A&A, 389, 115
- Dennett-Thorpe J., Scheuer, P. A. G., Laing, R. A., et al. 2002, MNRAS, 330, 609
- Eales, S., & Rawlings, S., 1996, ApJ, 460, 68
- Elvis, M. 2000, ApJ, 545, 63
- Fukugita, M., Ichikawa, T., Gunn, J. E., et al. 1996, AJ, 111, 1748
- Giroletti, M., Giovannini, G., & Taylor, G. B. 2005, A&A, 441, 89
- Giroletti, M., Giovannini, G., Taylor, G. B., et al. 2003, A&A, 399, 889
- Gopal-Krishna, & Wiita, P. J. 2000, A&A, 363, 507
- Gregg, M. D., Becker, R. H., Brotherton, M. S., et al. 2000, ApJ, 544, 142
- Gregg, M. D., Becker, R. H., & de Vries, W. 2006, ApJ, 641, 210
- Gregorini, L., Padrielli, L., Parma, P., & Gilmore, G. 1988, A&AS, 74, 107
- Gugliucci, N. E., Taylor, G. B., Peck, A. B., & Giroletti, M. 2005, ApJ, 622, 136

- Haas, M., Chini, R., Muller, S. A. H., Bertoldi, F., & Albrecht, M. 2006, *A&A*, 445, 115
- Hewett, P. C., & Foltz, C. B. 2003, *AJ*, 125, 1784
- Jeyakumar, S., Wiita, P. J., Saikia, D. J., & Hooda, J. S., 2005, *A&A*, 432, 823
- Jiang, D. R., & Wang, T. G. 2003, *A&A*, 397, L13
- Kunert, M., Marecki, A., Spencer, R. E., Kus, A. J., & Niezgoda J. 2002, *A&A*, 391, 47 (Paper I)
- Kunert-Bajraszewska, M., Marecki, A., Thomasson, P., & Spencer, R. E. 2005, *A&A*, 440, 93 (Paper II)
- Kunert-Bajraszewska, M., Marecki, A., & Thomasson, P. 2006, *A&A*, 450, 945 (Paper IV)
- Lipari, S. L., & Terlevich, R. J. 2006, *MNRAS*, 368, 1001
- Liu, F. K., 2004, *MNRAS*, 347, 1357
- Lowe, S. R., 2005, PhD thesis, University of Manchester
- Machalski, J., & Condon, J. J. 1983, *AJ*, 88, 143
- Machalski, J. 1998, *A&AS*, 128, 153
- Marecki, A., Spencer, R. E., & Kunert, M. 2003, *PASA*, 20, 46
- Marecki, A., Kunert-Bajraszewska, M., & Spencer, R. E. 2006, *A&A*, 449, 985 (Paper III)
- Menou, K., Vanden Berk, D. E., & Ivezić, Ž. 2001, *ApJ*, 561, 645
- Merritt, D., & Ekers, R. D. 2002, *Science*, 297, 1310
- Minns, A. R., & Riley, J. M. 2000, *MNRAS*, 318, 827
- Murgia, M., Fanti, C., Fanti, R., et al. 1999, *A&A*, 345, 769
- Murray, N., Chiang, J., Grossman, S. A., & Voit, G. M. 1995, *ApJ*, 451, 498
- O'Dea, C. P., & Baum, S. A. 1997, *AJ*, 113, 148
- Orienti, M., Dallacasa, D., Fanti C., et al. 2004, *A&A*, 426, 463
- Owsianik, I., Conway, J. E., & Polatidis, A. G. 1998, *A&A*, 336, L37
- Patnaik, A. R., Browne, I. W. A., Wilkinson, P. N., & Wrobel, J. M. 1992, *MNRAS*, 254, 655
- Phillips, R. B., & Mutel, R. L. 1982, *A&A*, 106, 21
- Polatidis, A. G., & Conway, J. E. 2003, *PASA*, 20, 69
- Pringle, J. E. 1997, *MNRAS*, 292, 136
- Rawlings, S., Willott, C. J., Hill, G. J., et al. 2004, *MNRAS*, 351, 676
- Readhead, A. C. S., Xu, W., Pearson, T. J., Wilkinson, P. N., & Polatidis, A. G. 1994, in *Compact Extragalactic Radio Sources*, NRAO Workshop, ed. J. A. Zensus, K. Kellermann, 17
- Readhead, A. C. S., Taylor, G. B., Xu, W., et al. 1996, *ApJ*, 460, 612
- Reynolds, C. S., & Begelman, M. C. 1997, *ApJ*, 487, L135
- Riley, J. M., & Warner, P. J. 1994, *MNRAS*, 269, 166
- Saikia, D. J., Jeyakumar, S., Salter, C. J., et al. 2001, *MNRAS*, 321, 37
- Schoenmakers, A. P., de Bruyn, A. G., Röttgering, H. J. A., van der Laan, & Kaiser, C. R. 2000, *MNRAS*, 315, 371
- Smith, J. A., Tucker, D. L., Kent, S., et al. 2002, *AJ*, 123, 2121
- Stanghellini, C., O'Dea, C. P., Dallacasa, D., et al. 2005, *A&A*, 443, 891
- Stoeck, J. T., Morris, S. L., Weymann, J. T., & Foltz, C. B. 1992, *ApJ*, 396, 487
- Taylor, G. B., Readhead, A. C. S., & Pearson, T. J. 1996, *ApJ*, 463, 95
- Waldram, E. M., Yates, J. A., Riley, J. M., & Warner, P. J. 1996, *MNRAS*, 282, 779
- Weymann, R. J., Morris, S. L., Foltz, C. B., & Hewett, P. C. 1991, *ApJ*, 373, 23
- White, R. L., Becker, R. H., Helfand, D. J., & Gregg, M. D. 1997, *ApJ*, 475, 479
- White, R. L., Helfand, D. J., Becker, R. H., Glikman, E., & de Vries, W. 2007, *ApJ*, 654, 99
- Willott, C. J., Rawlings, S., Blundell, K. M., & Lacy, M. 1999, *MNRAS*, 309, 1017
- Willott, C. J., Rawlings, S., Archibald, E. N., & Dunlop, J. S. 2002, *MNRAS*, 331, 435
- Willott, C. J., Rawlings, S., & Grimes, J. A. 2003, *ApJ*, 598, 909
- Wills, B. J., & Brotherton, M. S. 1995, *ApJ*, 448, L81
- Wills, B. J., Brandt, W. N., & Laor, A. 1999, *ApJ*, 520, L91
- Zhou, H., Wang, T., Wang, H., et al. 2006, *ApJ*, 639, 716

List of Objects

- '1045+352' on page 3
- '1049+384' on page 3
- '1056+316' on page 3
- '1059+351' on page 3
- '1126+293' on page 4
- '1132+374' on page 4
- '1302+356' on page 4
- '1407+369' on page 5
- '1425+287' on page 5
- '1627+289' on page 5